ENGINEERING RESEARCH JOURNAL (ERJ)
Vol. 1, No. 46 October 2020, pp.16-26
Journal Homepage: erj.bu.edu.eg

Prediction Of Hardness And Wear Behaviour Of Friction Stir Processed Cast A319 Aluminum Alloys Using Machine Learning Technique

Faisal F. S. Al-Enzi S.S. Mohammed

Mechanical Engineering Department, Faculty of Engineering at Shoubra, Benha University, Cairo, Egypt.

ABSTRACT

In the present investigation, the influences of the friction stir processing (FSP) on the microstructure, hardness and wear behaviour of cast A319 Al alloy were investigated. The influence of the FSP process parameters, namely, the tool rotational and traverse speeds as well as the number of processing passes on the aforementioned characteristics were evaluated. Machine learning (ML) artificial intelligence (AI) technique was used to develop models predict the hardness and wear rate of the friction stir (FS) processed A319 Al alloy. The results revealed that FSP significantly improved the microstructure, hardness and wear resistance of the as-cast A319 Al alloy. FSP eliminated the structural defects such as porosities and cavities found in the as-cast alloy. Also, the coarse Si particles found in the as-cast alloy were totally vanished and replaced with high density and fine Si particles which are more uniformly distributed in the FS processed zones. Such microstructural modifications resulted in an enhancement in the hardness and wear rate of the FS processed A319 Al alloy when compared with the as-cast alloy. The developed ML models showed high accuracy and can be used successfully to predict the hardness and wear rate of the FS processed A319 Al alloy. The models exhibited mean absolute error percentage (MAEP) of about 2.15%, and 2.3% for the hardness and wear rate, respectively.

KEYWORDS: Friction stir processing, A319, Wear rate, Microstructure, Hardness, Machine learning.

1. INTRODUCTION

FSP is a relatively new solid-state technique that was patented by Thomas et al. In 1991 based on the friction stir welding (FSW) technique [1]. It is mainly used for modification of the microstructure of the materials through severe localized plastic deformation [2]. The FSP is a green and energy-efficient technique because there are no fumes or deleterious gases, radiations or noises are emitted. Also, FSP does not change the size and the shape of the processed workpiece or produce residual stresses in it. FSP was used in transportation and ship industries like fabrication of frames, Al expulsions and seaward facilities [3]. There are several FSP process parameters e.g. the tool rotational speed, traverse speed, number of passes, tilt angle of the tool, the axial force as well as the material and design of the FSP tool. The choice of the proper FSP process parameters resulted in a satisfactory microstructural and hence mechanical characteristics of the processed zones [2-4].

Machine learning (ML) is a subdivision of artificial intelligent (AI) [5]. Unlike the other modelling techniques such as the analytical and numerical modelling, in ML, computational intelligence algorithms create connections between input (experimental data) and output (predicted data) without the necessity to know the physical behavior of the system under investigation. The ML was widely applied in the field of all industries. The ML was successfully used in the FSW field [6-8]. In contrast, the application of the ML in the field of FSP is rarely reported.

Nevertheless, the microstructural, mechanical and tribological characteristics of the friction stir (FS) processed A356 cast aluminum alloy were reported [9-12]. There is a lake of investigations regarding the influence of the FSP on the characteristics of other cast Al alloys especially A319 alloy [13,14]. The A319 Al alloy has excellent casting and machining characteristics. Corrosion resistance and weldability of this alloy are very good. Typical applications for this alloy are a wide variety of structural castings for engine parts, engine crankcases, gas and oil pans, and general commercial applications [15].

It is the present investigation, the influences of the FSP process parameters on the microstructural, mechanical and tribological characteristics of A319 cast Al alloy were studied. The ML technique was used to develop models that are capable to predict the aforementioned characteristics. Moreover, the analysis of variance statistical (ANOVA) approach was used to evaluate the influence of the FSP process parameters under investigation.

2. EXPERIMENTAL PROCEDURES

2.1. Materials

The A319 (Al-Si-Cu) cast Al alloy was used as base alloy. The chemical compositions of the A319 alloy are listed in Table 1. The A319 alloy was received in the form of large ingots. The ingots were cut, remelted, and poured in permanent mould at 650 ºC in the form of thick rectangular plates having dimensions of 25 mm (width) × 100 mm (length) × 12 mm (thickness).

Table 1. The chemical composition of the A319 cast Al alloy.

Alloy	Chemical compositions (wt%)								
	Si	Fe	Cu	Mg	Mn	Ni	Zn	Ti	Al
A319	6.32	0.31	3.20	0.001	0.002	0.002	0.011	0.006	Bal.

2.2. Friction Stir Processing

Figure 1 shows a schematic illustration of the FSP operation. The FSP was carried out using a FSP tool having cylindrical pin profile and the dimensions shown in Fig. 2. The tool are made from H13 tool steel. The FSP was performed using conventional milling machine. During FSP, the A319 cast Al plates were clamped rigidly on the milling machine bed using a vice. The FSP were conducted using at three different tool rotation speeds (TRS), three different traverse speeds (TS) and up to three FSP passes. In each pass, the tool is travelled along the same line as the previous one but in the opposite direction. This means that the advancing side (AS) of the pass became the retreating side (RS) in the later pass. Table 2 lists the FSP process parameters and their levels. During the FSP of the A319 alloy, the tilt angle was kept constant at 2º.

2.3. Microstructural Investigations

After FSP, samples were cut through the perpendicular direction of the FSP line using a diamond saw under water-cooling to minimize any effects from plastic deformation. The microstructural characteristics of FS processed cast Al alloy were investigated using optical microscope. The FS processed specimens were prepared for metallurgical investigations according to the standard procedures for specimen preparation for metallurgical investigation including grinding and polishing. Metallurgical specimens were ground under water using SiC emery papers of increasing fineness from 200 up to 1500 grit. After that, they were polished using 0.3µm alumina suspension and 0.25 µm diamond suspension. The primary Si particles size were measured using image analyzing techniques.

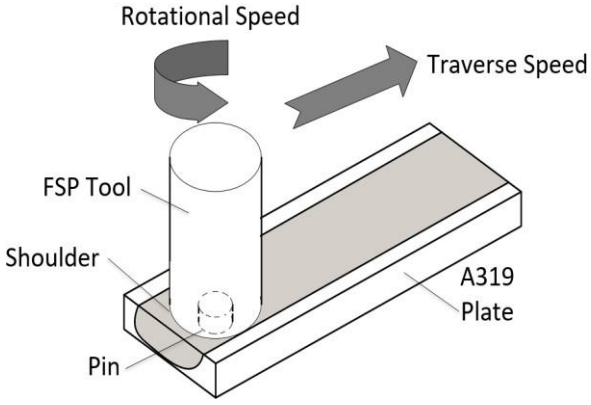

Figure 1. A schematic illustration of the FSP of A319 Al alloy.

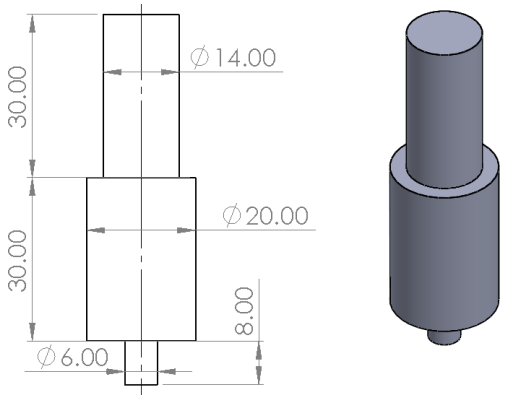

Figure 2. A schematic illustration of the FSP tool (Dimensions are in mm).

Table 2. The FSP parameters and their levels.

FSP Parameter	Symbol	Unit	Level		
			Min.	Mean	Max.
Tool Rotational Speed	TRS	rpm	1000	1400	1800
Traverse Speed	TS	mm/min.	40	60	80
Number of Passes	NP	-	1	2	3

2.4. Hardness Measurements

Vickers hardness measurements were performed in the traverse section along the center of the FS processed zone using an indenting load of 10 kg and a loading time of 10 seconds. A minimum of six readings were taken for each sample from the center of the stirred zone (SZ) and the average value was determined. Before the hardness measurements were performed the specimens were ground under water using SiC abrasive discs with increasing finness up to 600 grit.

2.5. Dry Sliding Wear Tests

Dry sliding wear tests were performed to evaluate the wear resistance of the FS processed A319 cast Al alloy and compare it with the wear resistance of the unprocessed A319 cast Al alloy. The wear tests were performed using the pin-on-ring wear testing machine. The counterface ring has a diameter of 200 mm is made from 316 stainless steel. The chemical analysis of the 316 stainless steel ring. The counterface ring has a hardness of about 80-90 BHN. During the wear experiments, the load and the rotating speed of the disc were kept constant at 20 kN and 300 rev/min. The maximum sliding distance is about 5 km. The duration of the experiment was controlled using a built-in stopwatch.

The specimens have square cross-section with a dimensions of 6 mm × 6 mm × 12 mm (height). The top surfaces of the FS processed samples were ground using SiC emery papers with increasing finness up to 1200 grit and cleaned with acetone. The specimens were then weighted before each experiment on a sensitive balance having an accuracy of 1×10^{-4} gm. After each wear experiment, the specimen is weighted again and the weight loss was calculated. For each test condition, at least three runs were performed and the average weight loss was calculated. The wear rate, in g/cm^2, was calculated using the following formula:-

$$\text{Wear rate} = \Delta W/A \quad \ldots(1)$$

Where, ΔW is weight loss (g), and A is area of exposed surface to the friction (mm^2).

2.6. Machine Learning (ML) Modelling

The Machine Learning (ML) modelling was performed to model the corrosion rate, hardness and wear rate of the FS processed zones as a function of FSP process parameters, typically the tool rotational speed, traverse speed and number of passes. The Support Vector Machines (SVM) method was used to perform the regression tasks by constructing nonlinear decision boundaries. Because of the nature of the feature space in which these boundaries are found, SVM can exhibit a large degree of flexibility in regression tasks of varied complexities. The Radial basis functions (RBF) SMV model was used. The accuracy of the developed ML models was determined using the Mean Absolute Error Percentage (MAEP) as follows:-

$$MAEP = \frac{1}{n}\sum_{i=1}^{n}\left|D_{exp} - D_{pre}\right| \times 100\% \quad \ldots(2)$$

Where D_{exp} is the experimental value of the hardness or wear rates, D_{pre} is the predicted values of the wear rates or hardness and n represents the number of samples.

3. RESULTS AND DISCUSSION

3.1. Microstructural Investigations

Figure 3 shows optical micrographs of the microstructure of as-cast A319 Al alloy. The microstructure of the as-cast A319 Al alloy consists mainly of α-Al primary dendrites and coarse acicular eutectic and primary coarse Si particles (Fig. 3a). It is clear that the primary Si particles was not homogeneous distribution throughout the α- Al matrix (Fig. 3b). The average size of the primary Si in the as-cast A319 Al alloy is approximately 52±15 μm. The as-cast A319 Al alloy showed a typical dendritic microstructure with a mean secondary dendrite arm spacing (SDAS) of about 95±12 μm. Several defects such as porosity or cavities with irregular shapes were observed in the microstructure of the as-cast A319 Al alloy (Fig. 3c). …(1)

(a) 50 × (b) 100 × (c) 50 ×

Figure 3. The microstructure of the as-cast A319 Al alloy.

It is important to remark that the boundaries of α-Al primary grains were very difficult to observe under the optical microscope. So, it was difficult to determine the size of the α-Al primary grains. Figures 4 shows typical microstructures of FS processed zones developed using different FSP process parameters. It is clear that the dendritic microstructure of the as-cast A19 alloy is totally nonexistent after FSP.

Moreover, the coarse Si particles were totally vanished and replaced with high density and fine Si particles which are more uniformly distributed in the FS processed zones. The microstructural changes may attribute to the stirring action produced by the tool during FSP. This action resulted in the breakup of the coarse Si particles to very fine particles. Also, the structural defects such as the porosities and cavities were eliminated in the FS processed regions.

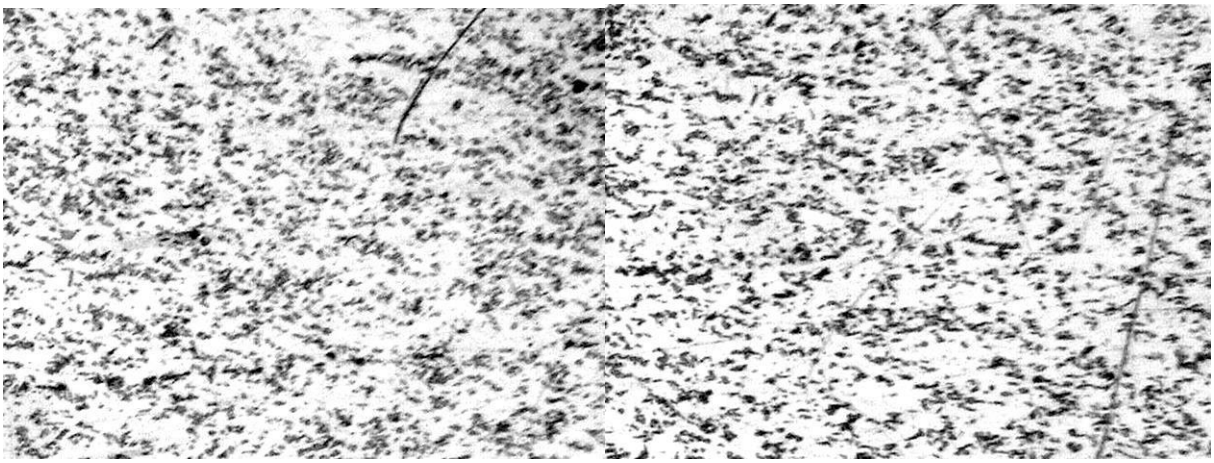

(a) 200× (b) 200×

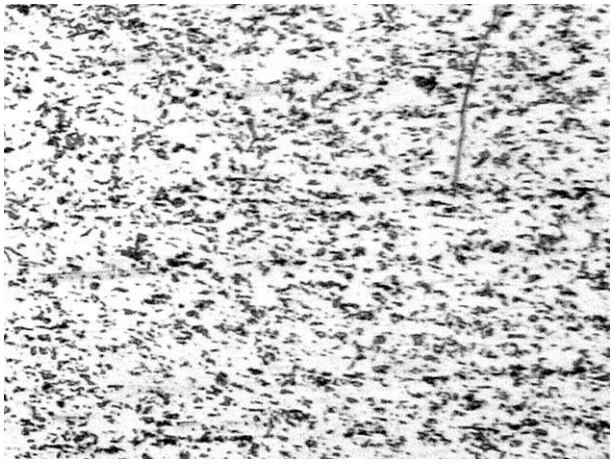

(c) 200×

Figure 4. The microstructure at the center of FS processed zone of the A319 Al-Si Alloy using constant tool rotational speed of 1400 rpm, single pass and traverse speeds of (a) 40 mm/min, (b) 60 mm/min and (c) 80 mm, respectively.

Figure 5 shows the variation of the Si particles mean size with the tool rotational speed at different traverse speeds and number of passes. The results revealed that increasing the tool rotational speed and/or the number of processing passes increasing the mean size of the Si particles. For example, at constant traverse speed of 80 mm/min and 1-pass, increasing the tool rotational speed from 1000 rpm to 1800 rpm increases the mean Si size from 5.2 µm to 8.7 µm. Also, at constant tool rotational speed of 1400 rpm and traverse speed of 40 mm/min, increasing the number of processing passes from 1 to 3 passes increasing the mean Si size from 8.9 µm to 10.8 µm. The results revealed also that after each processing pass the Si particles redistribute in the processing zone, which resulted in a better distribution and smaller size of the Si particles. In contrast, it has been found that increasing the traverse speed reduces the mean Si particles size. For example, at constant tool rotational speed and number of processing passes of 1400 rpm and 3-passes, increasing the traverse speed from 40 mm/min to 80 mm/min was found to reduce slightly the mean size of the Si particles from 10.8 µm to 9.3 µm.

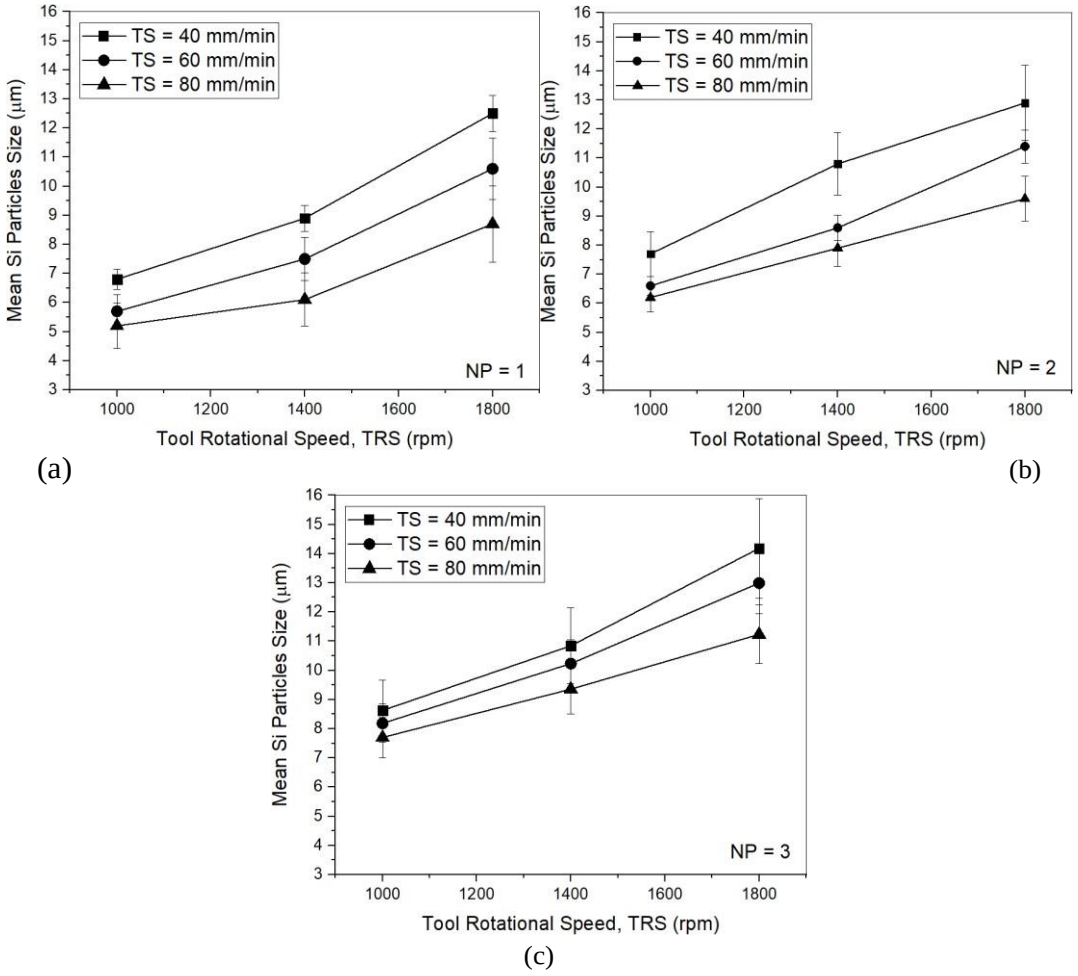

Figure 5. Variation of the Si particles size at the center of FS processed zone of A319 cast Al alloy with the tool rotational speed (TRS) at different traverse speed (TS) and (a) single pass NP=1, (b) double passes NP=2 and (c) three passes NP=3.

The maximum mean size of Si particles is about 14.1 μm was observed in the center of zone FS processed using tool rotational speed, traverse speed and number of processing passes of 1800 rpm, 40 mm/min and 3-passes, respectively. While the minimum mean size of Si particles is about 5.2 μm was observed in the center of zone FS processed using tool rotational speed, traverse speed and number of processing passes of 1000 rpm, 80 mm/min and single pass, respectively.

3.2. Hardness of the FS Processed Zones

Figure 6 shows the variation of the mean hardness with the rotational speed at different traverse speeds and number of passes. The results revealed that increasing the rotational speed and the number of passes increase the mean hardness in the FS processed zone. For example, at constant traverse speed of 40 mm/min and 1-pass, increasing the rotational speed from 1000 rpm to 1800 rpm increases the hardness from 42.1 to 52.3 VHN. While, at constant rotational speed of 1800 rpm and traverse speed of 60 mm/min, increasing the number of passes from 1 to 3 passes increasing the hardness from 48.2 to 53.6 VHN.

However, increasing the traverse speed reduces the mean hardness at the center of the FS processed zone. For example, at constant rotational speed and number of passes of 1000 rpm and 2-passes, increasing the traverse speed from 40 mm/min to 80 mm/min reduced the mean hardness from 44.6 to 37.5 VHN. The results revealed also that the maximum mean hardness was about 63.1 VHN and observed in zone FS processed using rotational speed, traverse speed and number of passes of 1800 rpm, 40 mm/min and 3-passes, respectively. While the minimum mean hardness was about 35.5 VHN and observed in the center of zone FS processed using rotational speed, traverse speed and number of passes of 1000 rpm, 80 mm/min and single pass, respectively.

The hardness of the base A319 Al as-cast alloy showed hardness values varying between 30.2 and 50.9 VHN with an average hardness value of about 42 VHN. The FS processed zones

showed more uniform hardness values distribution with lesser scatter. This may attribute to the finer and the more homogenous distribution of the Si particulates as well as the elimination of the structural defects in the FS processed zones when compared with the as-cast base alloy [16].

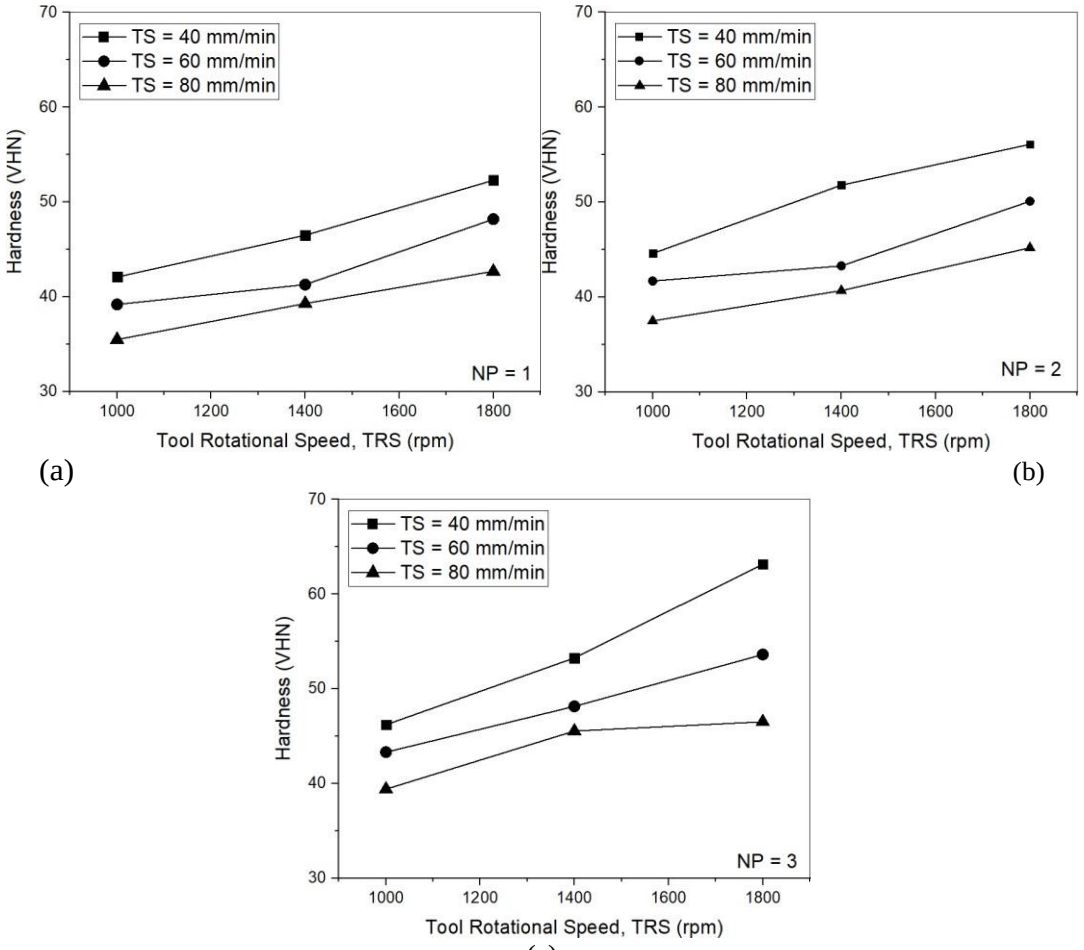

Figure 6. Variation of the hardness at the center of FS processed zone of A319 cast Al alloy with the tool rotational speed (TRS) at different traverse speed (TS) and (a) single pass NP=1, (b) double passes NP=2 and (c) three passes NP=3.

The increase of the mean hardness values at the center of the FS processed zones with increasing the tool rotational speed, number of processing passes as well as reducing the tool traverse speed, may attribute to the increase in the Si particles size exhibited at higher rotational speeds and number of processing passes as well as reducing the traverse speeds. The same observation regarding the effect of tool rotational speed on the hardness of cast Al alloys were reported by *Sima et al.* [17]. They reported that the hardness increases with increasing tool rotational speed. While *Tasi* and *Kao* [18] reported that the hardness increased with increasing tool rotational speed and/or decreasing the tool traverse speed. In contrast, *Mahmoud et al.* [19] showed that the mean hardness of the stirred zones increases with increasing the tool traverse speed and the number of passes, while decreases with increasing the tool rotational speed.

3.3. Wear Rate of the FS Processed Samples

The wear rate of the as-cast A319 Al alloy was about 130.56 mg/mm^2. The FS processed sample exhibited higher wear resistances than the as-cast alloy. Figure 7 illustrates the variations of the wear rate with the tool rotational speed at several traverse speeds and the number of processing passes. The results revealed that increasing the tool rotational speed and/or the number of processing passes reduce(s) the wear rate. In contrast, increasing the traverse speed increasing the wear rate of the FS processed A319 cast Al samples. The minimum wear rate was about 55.65 mg/mm^2 and observed in zone FS processed using rotational speed, traverse speed and number of passes of 1800 rpm, 40 mm/min and 3-passes, respectively. While the maximum wear rate was about 83.39 mg/mm^2 and observed samples FS processed using rotational speed, traverse speed and number of passes of 1000 rpm, 80 mm/min and

single pass, respectively. The comparison of the wear rate of the as-cast and FS processed A319 alloy showed that FSP increased the wear resistance of the alloy considerably by decreasing the weight loss due to the increase in hardness after FSP.

The results showed an increase in the hardness with increasing the tool rotational speed and number of passes and/or the reduction of the traverse speed. The correlation between the volume of the material removed and the hardness can be formulated using the well known Archard's equation [16,19]:

$$W = k\,(PL/H) \qquad \ldots(3)$$

Where: W is the volume of the material removed, k is a constant, P is the applied load, L is the sliding distance and H is the hardness of the material. Increasing the hardness of the materials reduces the volume of the material removed from the surface. The FS processed A319 samples showed higher hardness than the as-cast base alloy, which improved the wear resistance of the A319 alloy. Moreover, the presence of uniformly distributed and hard Si particles within the Al matrix as well as the elimination of structural defects such as cavities enable the alloy to withstand the applied loads (lessen deformation) and improves the wear resistance. The large Si particles found in as-cast allot can be removed from the surface of the specimens by the delamination wear process and work as third-body particles which increase the wear rates. Moreover, the removed Si particles leave voids on the surface, which reduces the ability of the alloy to carry on the applied load since the Al soft matrix will be in direct contact with the counterface. The possibility of the occurrence of stress concentrations around pores found in the as-cast A319 alloy increases the wear rates [19].

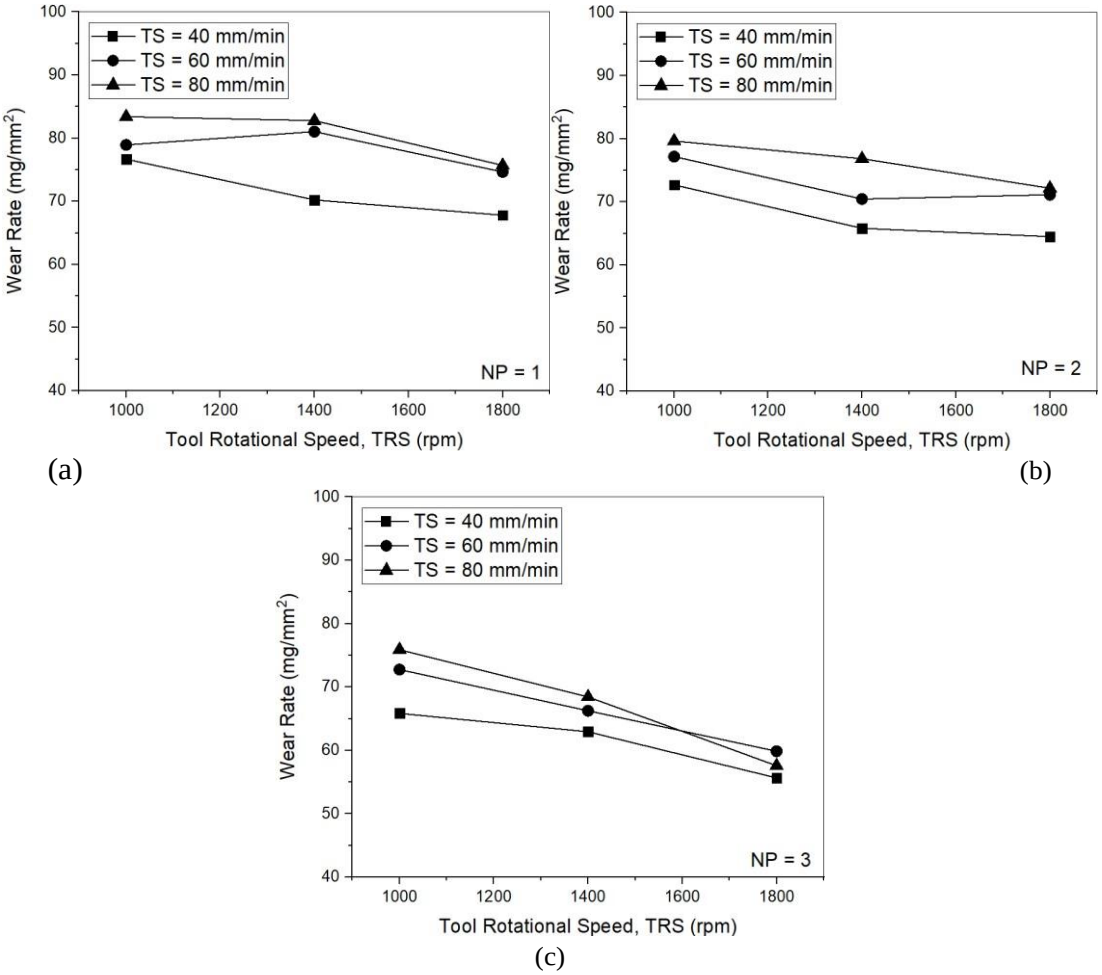

Figure 7. Variation of the wear rate of FS processed zone of A319 cast Al alloy with the tool rotational speed (TRS) at different traverse speed (TS) and (a) single pass NP=1, (b) double passes NP=2 and (c) three passes NP=3.

3.4. Machine Language Modelling Results

3.4.1. The ML Model for Predicting the Hardness

Figure 8 shows a plot for the actual (observed) vs predicted data. The MAEP of the developed model for the hardness at the center of the FS processed zone is about 2.15%. Figures 9 to 11 show surface plots developed from the ML model for the variation of the predicted hardness with the FSP process parameters.

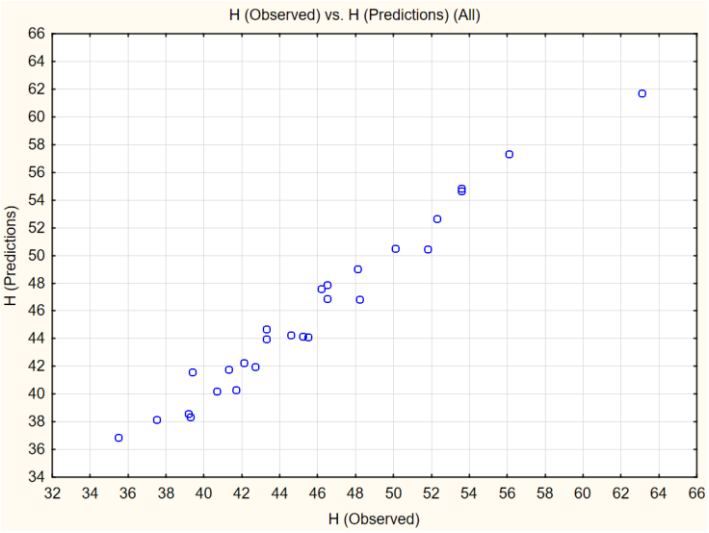

Figure 8. The predicted hardness vs. observed hardness.

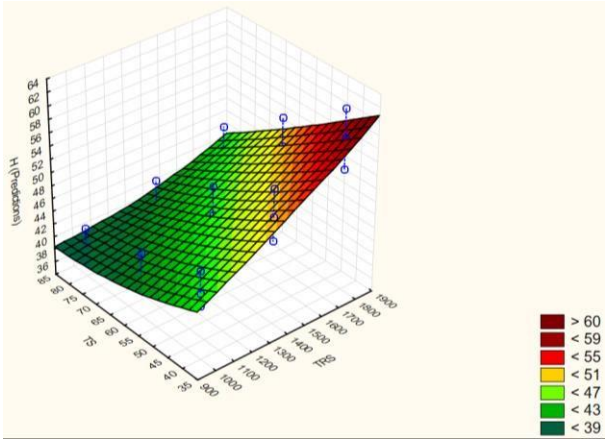

Figure 9. Surface plot for the variation of the predicted hardness (H) with the tool rotational speed (TRS) and traverse speed (TS).

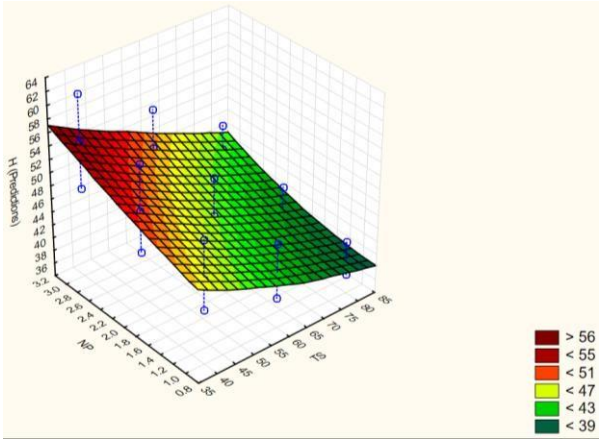

Figure 10. Surface plot for the variation of the predicted hardness (H) with the traverse speed (TS) and number of passes (NP).

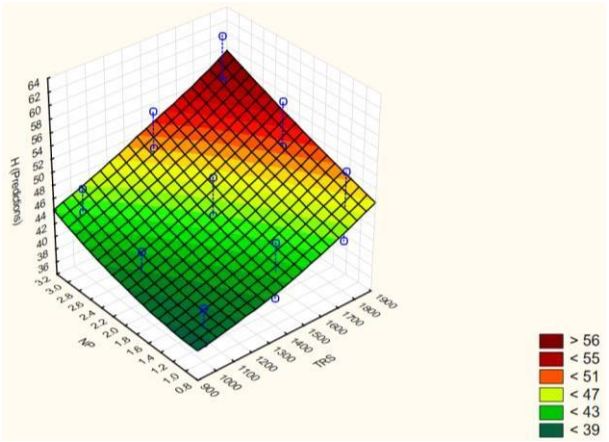

Figure 11. Surface plot for the variation of the predicted hardness (H) with the tool rotational speed (TRS) and number of passes (NP).

3.4.2. The ML Model for Predicting the Wear Rate

Figure 12 shows a plot for the observed vs predicted data for the wear rate. The MAEP of the developed model for the wear rate is about 2.3%. Figures 13 to 15 show surface plots developed from the ML model for the variation of the predicted wear rates with the FSP process parameters.

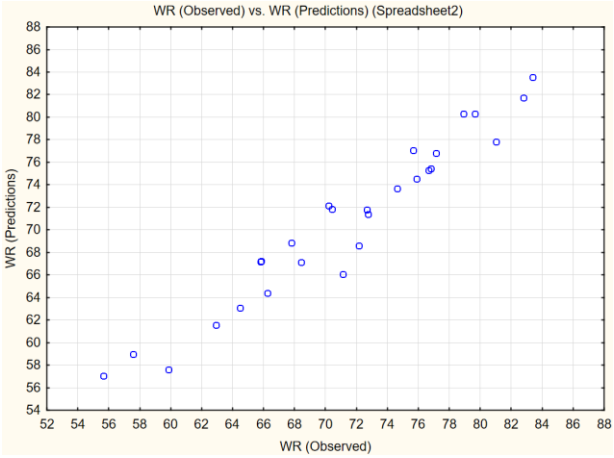

Figure 12. The predicted wear rates vs. observed wear rates.

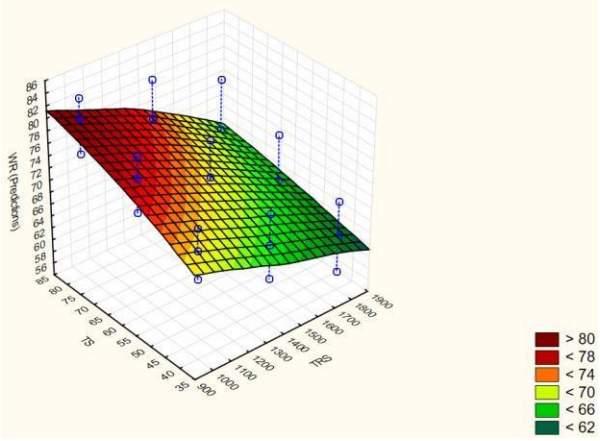

Figure 13. Surface plot for the variation of the predicted wear rate (WR) with the tool rotational speed (TRS) and traverse speed (TS).

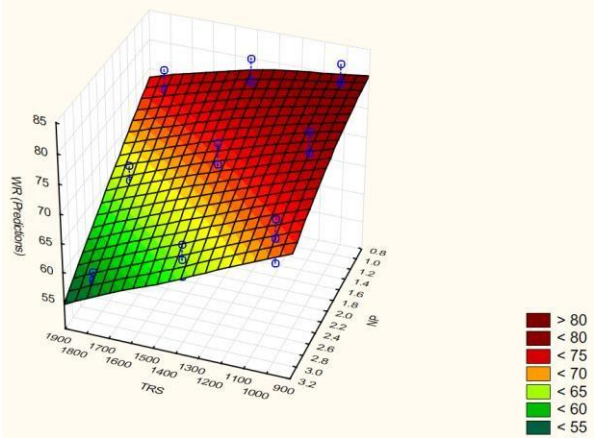

Figure 14. Surface plot for the variation of the predicted wear rate (WR) with the tool rotational speed (TRS) and number of passes (NP).

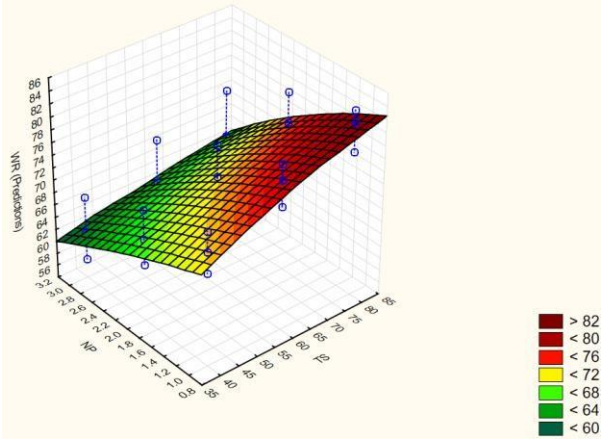

Figure 15. Surface plot for the variation of the predicted wear rate (WR) with the traverse speed (TS) and number of passes (NP).

In the present investigation, the ML developed models for predicting the hardness, wear rate and corrosion rate was successfully used. Comparison of experimental results with the data predicted from ML models has shown its high level of agreement between prediction and test data.

4. CONCLUSIONS

1. The average size of the primary Si in the as-cast A319 Al alloy was about 52±15 μm. After FSP, the coarse Si particles were totally vanished and replaced with high density and fine Si particles which are more uniformly distributed in the FS processed zones. Also the structural defects such as the porosities and cavities were eliminated in the FS processed regions. Increasing the tool rotational speed and/or the number of processing passes increasing the mean size of the Si particles. In contrast, it has been found that increasing the traverse speed reduces the mean Si particles size. The maximum and minimum values mean size of Si particles are about 14.1 μm and 5.2 μm, respectively.
2. The hardness of the base A319 Al as-cast alloy varies between 30.2 and 50.9 VHN with an average hardness value of about 42 VHN. The FS processed zones showed more uniform hardness values distribution with lesser scatter. The maximum and minimum mean hardness were about 63.1 VHN and 35.5 VHN, respectively. Increasing the rotational speed and the number of passes increase the mean hardness in the FS processed zone. However, increasing the traverse speed reduces the mean hardness at the center of the FS processed zone.
3. The FSP A319 samples exhibited higher wear resistance than the A319 as-cast alloy. Increasing the tool rotational speed and/or the number of processing passes reduce(s) the wear rate. In contrast, increasing the traverse speed increasing the wear rate of the FS processed A319 cast Al samples.
4. The effectivness of the developed machine learning models for predicting the hardness and wear rates of the FSP zones was approved. The mean absolute error percentage (MAEP) of the developed models for the hardness and wear rate were about 2.15% and 2.3%, respectively.

REFERENCES

[1] W.M. Thomas, E.D. Nicholas, J.C. Needdham, M.G. Much, P. Templesmith,C.J. Dawes, “Friction-stir Butt Welding”, GB Patent Application, No 9125978.8, 1991.

[2] Harvinder Singh and Rajdeep Singh, “A Review Study of Friction Stir Processing of Aluminum Alloy”, Asian Review of Mechanical Engineering, 7(2), 2018, pp. 46-49.

[3] M. Puviyarasan, L. Karthikeyan, C. Gnanavel, K. Dhineshkumar, “A critical review on friction stir based processes”, Advances in Engineering Research (AER), volume 142, 2018, pp. 258-266.

[4] Uday Sen, Kulbhushan Sharma, “Friction Stir Processing of Aluminum Alloys: A Literature Survey”, International Journal of Scientific Research in Science, Engineering and Technology (IJSRSET), 2(2), 2016, pp. 2395-1990.

[5] E. Alpaydin, “Introduction to Machine Learning”, Second Edition. The MIT Press Cambridge, Massachusetts London, England, 2010.

[6] S. Verma, M. Gupta, J. P. Misra, “Performance evaluation of friction stir welding using machine learning approaches”, MethodsX, 5, 2018, pp. 1048– 1058.

[7] Armansyah, W. Astuti, “Development of Prediction System Model for Mechanical Property in Friction Stir Welding Using Support Vector Machine (SVM)”, Journal of Mechanical Engineering, 5(5), 2018, pp. 216–225.

[8] Y. Du, T. Mukherjee, T. DebRoy, “Conditions for void formation in friction stir welding from machine learning”, npj Computational Materials, 5(1), 2019, pp. 1-8.

[9] G. Madhusudhan Reddy, K. Srinivasa Rao, “Enhancement of wear and corrosion resistance of cast A356 aluminium alloy using friction stir processing”, Transactions of The Indian Institute of Metals, 63, 2010, pp. 793-798.9.

[10] A.O. Shiba, S. S. Mohamed, T.S. Mahmoud, “Influence of Friction Stir Processing on the Microstructural, Hardness and Tribological Characteristics of A356 Cast Aluminium Alloy”, steel-grips, 2018, pp. 24-31.

[11] S.R. Sharma, Z.Y. Ma, R.S. Mishra, “Effect of friction stir processing on fatigue behaviour of A356 alloy”, Scripta Materialia, 51, 2004, pp. 237-241.

[12] G. Madhusudhan Reddy, K. Srinivasa Rao, “Enhancement of wear and corrosion resistance of cast A356 aluminium alloy using friction stir processing”, Transactions of The Indian Institute of Metals, 63, 2010, pp. 793-798.

[13] M.L. Santella, T. Engstrom, D. Storjohann, and T.Y. Pan, “Effects of friction stir processing on mechanical properties of the cast aluminum alloys A319 and A356”, Scripta Mater., 53, 2005, pp. 201–206.

[14] L. Karthikeyan, V.S. Senthil Kumar, K.A. Padmanabhan, “On the role of process variables in the friction stir processing of cast aluminum A319 alloy”, Materials and Design, 31, 2010, pp. 761–771.

[15] Sepehrband Panthea, Ghasemi Hamid, “Improved properties of A319 aluminum casting alloy modified with Zr”, Materials Letters, 60, 2006, pp. 2606-2610.

[16] T.S. Mahmoud, S.S. Mohamed, “Improvement of microstructural, mechanical and tribological characteristics of A413 cast Al

alloys using friction stir processing", Materials Science and Engineering A, 558, 2012, pp. 502-509.

[17] Sima Ahmad Alidokhta, Amir Abdollah-zadeh, Soheil Soleymani, Tohid Saeidb, Hamid Assadia, "Evaluation of microstructure and wear behavior of friction stir processed cast aluminum alloy", Mater. Charact., 63, 2012, pp. 90- 97.

[18] F.Y. Tsai and P.W. Kao, "Improvement of mechanical properties of a cast Al-Si base alloy by friction stir processing", Materials Letters, 80, 2012, pp. 40-42.

[19] T.S. Mahmoud, "Surface modification of A390 hypereutectic Al–Si cast alloys using friction stir processing", Surface & Coatings Technology, 228, 2013, 209- 220.